Published OnlineFirst August 4, 2011; DOI:10.1158/1078-0432.CCR-11-1477

Clinical Cancer Research

CCR Translations
Commentary on Preis et al., p. 5812

microRNA-10b: A New Marker or the Marker of Pancreatic Ductal Adenocarcinoma?

Tetsuro Setoyama[1,4], Xinna Zhang[2,3], Shoji Natsugoe[4], and George A. Calin[1,3]

microRNA-10b (miR-10b) expression in pancreatic ductal adenocarcinoma (PDAC), as identified by *in situ* hybridization, is highly correlated with cancer diagnosis, therapy response, and prognosis. If these findings are further confirmed in prospective studies, miR-10b could be used to improve the management of PDAC and decrease the mortality rate of this deadly cancer. *Clin Cancer Res; 17(17); 5527–9.* ©*2011 AACR.*

In this issue of *Clinical Cancer Research*, Preis and colleagues (1) report that the level of microRNA-10b (miR-10b) expression, as found using *in situ* hybridization (ISH) of endoscopic ultrasonography (EUS)–guided fine needle aspiration (FNA) biopsy samples, was significantly correlated with response to neoadjuvant therapy and outcome in pancreatic ductal adenocarcinoma (PDAC).

This study is important for several reasons. First, the authors wisely focused on a deadly type of cancer, PDAC, which is the fourth leading cause of cancer death and the second most common gastrointestinal malignancy in the United States. The median survival duration of PDAC patients is 4.4 months, and the 5-year survival rate is around 4% for all PDAC patients (2). At present, no established biomarkers for early diagnosis and prognosis exist; therefore, it is imperative that we find new predictors for both patients and clinicians. Carcinoembryonic antigen (CEA) and cancer antigen 19-9 (CA19-9) are regarded worldwide as standard adjunctive markers, but their levels are also elevated in benign and other malignant conditions; thus, they are not recommended for diagnosis or prognosis by the American Society of Clinical Oncology (3).

Second, the identified gene, *miR-10b*, makes functional sense as being intimately linked to the mechanism of metastasis, the cause of most PDAC deaths. microRNAs (miRNA) are 19- to 25-nucleotide (nt) noncoding RNAs (ncRNA) and are already classic examples of RNA molecules that do not codify for proteins. By degrading or blocking translation of mRNA targets, these miRNAs can regulate a large part of the mammalian genome, including genes involved in metastases (4). miRNAs are also involved in the initiation and progression of human cancers (5) and can behave as oncogenes or tumor suppressors (4). Among miRNAs, miR-10b was the first that was found, by Ma and colleagues (6), to be correlated with metastasis in breast cancer. It is induced by the epithelial–mesenchymal transition–related transcription factor Twist and suppresses HOXD10, which represses several genes that contribute to cell migration and extracellular matrix remodeling in breast cancer, RhoC, urokinase plasminogen activator receptor, a3-integrin, and MT1–matrix metalloproteinase (MMP; ref. 6). Another target of miR-10b is Kruppel-like factor 4 (KLF4), which acts as a transcriptional factor. In esophageal cancer cells, miR-10b was found to directly suppress KLF4, promoting cancer invasion (7). One target of miR-10b is the tumor suppressor neurofibromin; in neurofibromatosis malignant peripheral nerve sheath tumor cells, miR-10b directly suppresses the mRNA of neurofibromin, and RAS signaling in these cells is activated (8). In contrast, T lymphoma invasion and metastasis 1 (TIAM1) was identified as an additional target gene for miR-10b; silencing TIAM1 caused suppression of breast cancer cell migration (Fig. 1A; ref. 9).

Third, the authors used adequate material for the study. EUS-FNA is highly accurate at identifying patients with suspected PDAC, especially when other modalities have failed, and has rare complications (10). EUS-FNA biopsy specimens are as reliable as surgical tissues, with a reported positive predictive value, negative predictive value, and accuracy rate of 99%, 64%, and 84%, respectively. EUS-FNA biopsy is a sensitive method, but false-negative cases must also be evaluated (10). EUS-FNA biopsy is done before therapy, allowing the clinician to predict response or outcome. Preis and colleagues used a highly sensitive fluorescence-based ISH technique combined with immunohistochemical analysis with cytokeratin 19 to identify epithelial cells in EUS-FNA biopsy specimens. This method was not time consuming and enabled them to evaluate the

Authors' Affiliations: Departments of [1]Experimental Therapeutics and [2]Cancer Biology and [3]Center for RNA Interference and Non-Coding RNAs, The University of Texas MD Anderson Cancer Center, Houston, Texas; [4]Department of Surgical Oncology and Digestive Surgery, Graduate School of Medical and Dental Sciences, Kagoshima University, Kagoshima, Japan

Corresponding Author: George A. Calin, Department of Experimental Therapeutics, Unit 36, The University of Texas MD Anderson Cancer Center, Houston, TX 77030. Phone: 713-792-5461; Fax: 713-745-4528; E-mail: gcalin@mdanderson.org

doi: 10.1158/1078-0432.CCR-11-1477

©2011 American Association for Cancer Research.

Downloaded from clincancerres.aacrjournals.org on May 23, 2012
Copyright © 2011 American Association for Cancer Research

Published OnlineFirst August 4, 2011; DOI:10.1158/1078-0432.CCR-11-1477

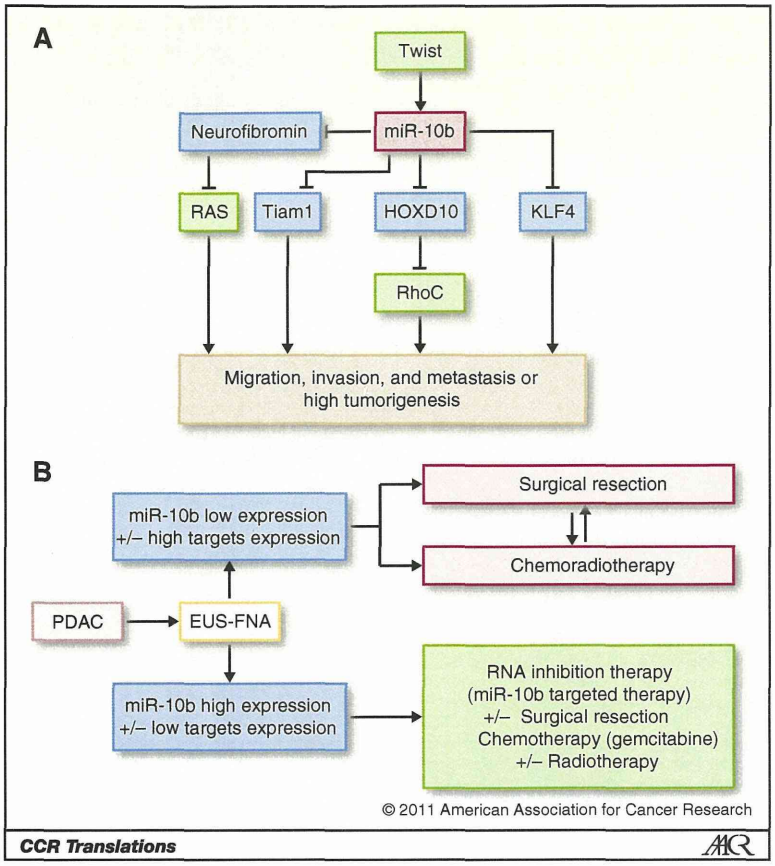

Figure 1. Possible future PDAC *management decisions using* ISH of miR-10b expression. A, molecular mechanism of miR-10b action; B, treatment decisions based on miR-10b and target expression.

spatial cancer-specific expression of miR-10b. Another method that can select only cancer cells, laser capture microdissection (11), is more time consuming and technically demanding than the combination of ISH and immunohistochemical analysis.

Finally, and most significantly, these authors' findings have high translation potential. They initially determined the expression of miR-10b, miR-21, miR-155, miR-196a, and miR-210 using ISH in 10 resected PDAC formalin-fixed, paraffin-embedded clinical specimens and 3 non-cancerous tissues. The authors found that miR-10b was the most frequently and consistently upregulated in cancer cells. They then used ISH to determine miR-10b expression in 95 PDAC and 11 benign EUS-FNA biopsy samples. In cancer tissue, miR-10b expression (measured automatically as mean fluorescence intensity) was about 5 times higher than that in benign tissue. miR-10b expression was significantly useful for cancer diagnosis. Subsequently, they compared miR-10b expression and the response of neoadjuvant chemoradiotherapy. They found significantly lower miR-10b levels in tumors that responded than in those that did not. In addition, they detected significantly lower miR-10b levels in resectable than in unresectable tumors. These findings indicate that miR-10b can be used to predict response to therapy. Thereafter, the authors found a significantly longer time to metastasis in patients with low miR-10b expression. Moreover, patients with low miR-10b expression had longer overall survival durations than did patients with high expression, for all stages; durations were even longer for stages I and II. These results suggest that miR-10b could be predictive of prognosis. It is clear that further studies to identify the critical targets of miR-10b in pancreatic cancer will also identify other pathways to target, either alone or in combination with chemotherapy.

One of the most significant findings of this study is the value of miR-10b for use in therapeutic decision making (Fig. 1B). Preis and colleagues (1) found that patients with low miR-10b expression experienced relatively better responses to gemcitabine-based neoadjuvant therapy and better prognoses. The best treatment for patients with unfavorably high miR-10b expression will be the most difficult decision in clinical practice. New alternative therapies, including miR-10b–targeted therapy, are needed. Many miRNAs have been reported to be oncogenic or suppressive, but few *in vivo* therapeutic advances have been made. Researchers have evaluated the use of

Downloaded from clincancerres.aacrjournals.org on May 23, 2012
Copyright © 2011 American Association for Cancer Research

Published OnlineFirst August 4, 2011; DOI:10.1158/1078-0432.CCR-11-1477

antagomirs as *in vivo* miRNA antagonists; antagomirs are a type of chemically engineered, cholesterol-conjugated antisense RNA oligonucleotide (12). A miR-10b antagomir was evaluated in a 4T1 mouse mammary tumor metastasis model. Ma and colleagues found that antagomir-10b prevents metastatic dissemination of cancer cells from the primary tumor but does not affect late stages of the metastatic process, when tumor cells have disseminated (12).

An important question is whether detection of miR-10b expression by ISH is ready for use in clinical practice. This study was done at a single institution and was retrospective; its findings must be confirmed in a multi-institutional prospective clinical trial. Clearly, cooperation and support among clinical surgeons, oncologists, pathologists, and molecular scientists is essential. miRNA detection with combined ISH and immunohistochemical staining could be challenging when the miRNAs are not well expressed. Furthermore, staining for the expression characterization of known target genes, in addition to specific miRNAs, could improve prediction accuracy (Fig. 1B). If the findings of this study are confirmed, they will be of great help toward developing a clinical strategy to select PDAC patients who will experience a response to neoadjuvant therapy and may experience a better outcome.

Disclosure of Potential Conflicts of Interest

No potential conflicts of interest were disclosed.

Acknowledgments

The authors thank Ann Sutton (Department of Scientific Publications, MD Anderson Cancer Center) for her help with the editing of this manuscript.

Grant Support

G.A. Calin is supported as a Fellow of the University of Texas MD Anderson Research Trust, as a University of Texas System Regents Research Scholar, and by the CLL Global Research Foundation. Work in Dr. Calin's laboratory is supported in part by the NIH; a Department of Defense Breast Cancer Idea Award; developmental research awards in Breast Cancer, Ovarian Cancer, Brain Cancer, Multiple Myeloma, and Leukemia SPOREs; a 2009 Seena Magowitz–Pancreatic Cancer Action Network AACR Pilot Grant; and the Arnold Foundation.

Received July 7, 2011; accepted July 21, 2011; published OnlineFirst August 4, 2011.

References

1. Preis M, Gardner TB, Gordon SR, Pipas MJ, Mackenzie TA, Klein EE, et al. microRNA-10b expression correlates with response to neoadjuvant therapy and survival in pancreatic ductal adenocarcinoma. Clin Cancer Res 2011;17:5812–21.
2. Bilimoria KY, Bentrem DJ, Ko CY, Ritchey J, Stewart AK, Winchester DP, et al. Validation of the 6th edition AJCC Pancreatic Cancer Staging System: report from the National Cancer Database. Cancer 2007;110:738–44.
3. Locker GY, Hamilton S, Harris J, Jessup JM, Kemeny N, Macdonald JS, et al. ASCO. ASCO 2006 update of recommendations for the use of tumor markers in gastrointestinal cancer. J Clin Oncol 2006;24:5313–27.
4. Nicoloso MS, Spizzo R, Shimizu M, Rossi S, Calin GA. MicroRNAs—the micro steering wheel of tumour metastases. Nat Rev Cancer 2009;9:293–302.
5. Calin GA, Croce CM. MicroRNAs and chromosomal abnormalities in cancer cells. Oncogene 2006;25:6202–10.
6. Ma L, Teruya-Feldstein J, Weinberg RA. Tumour invasion and metastasis initiated by microRNA-10b in breast cancer. Nature 2007;449:682–8.
7. Tian Y, Luo A, Cai Y, Su Q, Ding F, Chen H, et al. MicroRNA-10b promotes migration and invasion through KLF4 in human esophageal cancer cell lines. J Biol Chem 2010;285:7986–94.
8. Chai G, Liu N, Ma J, Li H, Oblinger JL, Prahalad AK, et al. MicroRNA-10b regulates tumorigenesis in neurofibromatosis type 1. Cancer Sci 2010;101:1997–2004.
9. Moriarty CH, Pursell B, Mercurio AM. miR-10b targets Tiam1: implications for Rac activation and carcinoma migration. J Biol Chem 2010;285:20541–6.
10. Eloubeidi MA, Chen VK, Eltoum IA, Jhala D, Chhieng DC, Jhala N, et al. Endoscopic ultrasound-guided fine needle aspiration biopsy of patients with suspected pancreatic cancer: diagnostic accuracy and acute and 30-day complications. Am J Gastroenterol 2003;98:2663–8.
11. Fujita H, Ohuchida K, Mizumoto K, Itaba S, Ito T, Nakata K, et al. High EGFR mRNA expression is a prognostic factor for reduced survival in pancreatic cancer after gemcitabine-based adjuvant chemotherapy. Int J Oncol 2011;38:629–41.
12. Ma L, Reinhardt F, Pan E, Soutschek J, Bhat B, Marcusson EG, et al. Therapeutic silencing of miR-10b inhibits metastasis in a mouse mammary tumor model. Nat Biotechnol 2010;28:341–7.

Downloaded from clincancerres.aacrjournals.org on May 23, 2012
Copyright © 2011 American Association for Cancer Research

Provided for non-commercial research and education use.
Not for reproduction, distribution or commercial use.

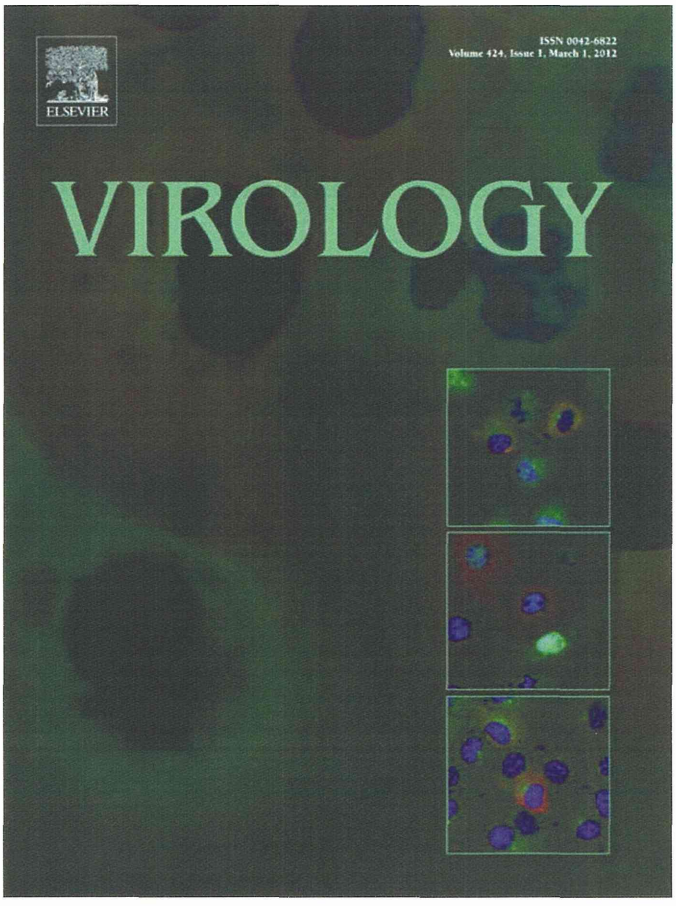

This article appeared in a journal published by Elsevier. The attached copy is furnished to the author for internal non-commercial research and education use, including for instruction at the authors institution and sharing with colleagues.

Other uses, including reproduction and distribution, or selling or licensing copies, or posting to personal, institutional or third party websites are prohibited.

In most cases authors are permitted to post their version of the article (e.g. in Word or Tex form) to their personal website or institutional repository. Authors requiring further information regarding Elsevier's archiving and manuscript policies are encouraged to visit:

http://www.elsevier.com/copyright

author's personal copy

Virology 424 (2012) 56–66

Contents lists available at SciVerse ScienceDirect

Virology

journal homepage: www.elsevier.com/locate/yviro

O-sulfate groups of heparin are critical for inhibition of ecotropic murine leukemia virus infection by heparin

Yohei Seki [a], Misaho Mizukura [a], Tomomi Ichimiya [a], Yasuo Suda [b], Shoko Nishihara [a], Michiaki Masuda [c], Sayaka Takase-Yoden [a,*]

[a] *Department of Bioinformatics, Faculty of Engineering, Soka University, Hachioji, Tokyo 192-8577, Japan*
[b] *Graduate School of Science and Engineering, Kagoshima University, Kagoshima 890-8580, Japan*
[c] *Department of Microbiology, Dokkyo Medical University School of Medicine, Tochigi 321-0293, Japan*

ARTICLE INFO

Article history:
Received 3 September 2011
Returned to author for revision
27 November 2011
Accepted 28 November 2011
Available online 9 January 2012

Keywords:
Env protein
Heparin
Murine leukemia virus
Sulfation
Surface plasmon resonance

ABSTRACT

There is increasing evidence that soluble glycosaminoglycans such as heparin can interfere with the infectivity of various viruses, including ecotropic murine leukemia viruses (MLVs). The ecotropic MLV, Friend MLV (F-MLV) and the neuropathogenic variants A8 MLV and PVC-211 MLV, were susceptible to heparin-mediated inhibition of infection of NIH 3T3 cells. To investigate the interaction between the envelope glycoprotein (Env) of MLV and heparin, we prepared vesicular stomatitis virus-based pseudotyped viruses carrying the Env of F-, A8, or PVC-211 MLVs. Surface plasmon resonance analyses indicated that the Env of A8 and PVC-211 MLVs had a higher binding activity to heparin than that of F-MLV. We examined the influence of *N*- or *O*-sulfation of heparin on binding activity to Env and on the inhibition of the infectivity of MLV and pseudotyped viruses carrying Env. This analysis indicated that the *O*-sulfate groups of heparin play a major role in determining Env-dependent inhibitory effects.

© 2011 Elsevier Inc. All rights reserved.

Introduction

Previous studies have shown that soluble glycosaminoglycans (GAGs), such as heparin, inhibit the infectivity of ecotropic murine leukemia virus (MLV) (Batra et al., 1997; Guibinga et al., 2002; Jinno-Oue et al., 2001; Le Doux et al., 1996, 1999; Masuda et al., 1997; Walker et al., 2002). Jinno-Oue et al. (2001) found that heparin influences Env-dependent attachment of the virus to the cell surface. By contrast, Walker et al. (2002) and Guibinga et al. (2002) reported that heparin inhibits Env-independent interaction of MLV with target molecules on the cell surface. Infection by ecotropic MLV is mediated by the binding of the viral Env protein to the rodent ortholog of cationic amino acid transporter 1 (CAT-1), which serves as the specific cellular receptor (Albritton et al., 1989; Kim et al., 1991; Wang et al., 1991). Although the Env-receptor interaction appears to be required for membrane fusion and entry of the viral capsid, it has been reported that initial attachment of a retroviral particle to the cell surface can take place in a receptor-independent manner (Guibinga et al., 2002; Pizzato et al., 1999; Walker et al., 2002). The fact that soluble GAGs, such as heparin, inhibit MLV infectivity suggests that cell surface GAGs, such as heparan sulfate, might be involved in the initial attachment (Batra et al., 1997; Guibinga et al., 2002; Jinno-Oue et al., 2001; Le Doux et al., 1996, 1999; Masuda et al., 1997; Walker et al., 2002). Similarly, it has been shown that infection by other enveloped viruses, such as herpes viruses (Neyts et al., 1992; Secchiero et al., 1997; WuDunn and Spear, 1989), respiratory syncytial virus (Krusat and Streckert, 1997) and human immunodeficiency virus (HIV) (Mondor et al., 1998; Patel et al., 1993), are inhibited by heparin, and that cell surface attachment of these viruses involves cell surface GAGs. Thus, the interaction of viral particles with soluble and cell surface GAGs is an important issue for virology in general.

In the present study, we initially investigated the influence of heparin on infection of ecotropic MLVs including Friend MLV (F-MLV) clone 57 (Oliff et al., 1980) and its neuropathogenic variants, A8 MLV (Takase-Yoden and Watanabe, 1997; Watanabe and Takase-Yoden, 1995) and PVC-211 MLV (Kai and Furuta, 1984; Masuda et al., 1992). The infection of neonatal rats with A8 or PVC-211 MLV induces spongiform neurodegeneration without inflammatory infiltrates. The primary determinant for neuropathogenicity of these viruses has been identified as Env. Comparison of the amino acid sequences of A8-Env and PVC-211-Env showed that only 3 of the 676 amino acids differ. F-MLV is non-neuropathogenic and F-Env shows differences at 26 of the 676 amino acids compared to A8-Env. Here, we performed surface plasmon resonance (SPR) analyses to compare the binding activities to heparin of pseudotyped viral particles carrying Env of ecotropic MLVs. To our knowledge, this is the first time that SPR technology has been applied in a quantitative analysis of

* Corresponding author. Fax: +81 42 691 2375.
E-mail address: takase@soka.ac.jp (S. Takase-Yoden).

0042-6822/$ – see front matter © 2011 Elsevier Inc. All rights reserved.
doi:10.1016/j.virol.2011.11.030

the interaction between viral particles carrying MLV Env and heparin. Heparin is a linear polysaccharide composed of α1-4 linked disaccharide repeating units. The most common unit contains 2-*O*-sulfated iduronic acid and 6-*O*-sulfated, *N*-sulfated glucosamine. The negatively-charged sulfate groups of heparan sulfate (which is structurally related to heparin) are thought to play an important role in its biological activity, such as fibroblast growth factor (FGF) signaling, and to act as an entry receptor for herpes simplex virus type 1 (Capila and Linhardt, 2002; Copeland et al., 2008; Shukla et al., 1999; Xia et al., 2002; Ye et al., 2001). We also examined the relative importance of *N*- or *O*-sulfation of heparin for its inhibitory effects on infection by ecotropic MLVs and on the binding activities to viral particles using chemically modified heparins: *N*-acetylheparin (NA-H), which has diminished *N*-sulfation; de-*N*-sulfated heparin (dNS-H), which completely lacks *N*-sulfation; and *N*-acetyl-de-*O*-sulfated heparin (NAdOS-H), which has markedly diminished *N*-sulfation and completely lacks *O*-sulfation. Taken together, the present investigations have characterized the inhibitory activities of heparin against ecotropic MLV infection of NIH 3T3 cells, while the SPR analysis showed that the binding activity of ecotropic MLV with heparin may be determined by Env amino acid sequences. We also demonstrate that the *O*-sulfate groups of heparin play a major role in inhibiting the infectivity of ecotropic MLV on cells in an Env-dependent manner. The possible mechanisms of the inhibition of heparin against viral infection and the implications of heparan sulfate on the cell surface are discussed.

Results

Inhibition of ecotropic MLV infection by heparin and its derivatives

We compared the effects of heparin and its derivatives on the infectivity of F-, A8, and PVC-211 MLVs using viruses that had been pre-incubated with various concentrations of heparin, or one of the derivatives, in the absence of polybrene. After this pre-incubation step, the virus-heparin or virus-derivative mixture was inoculated onto NIH 3T3 cells at a multiplicity of infection (MOI) of 1 in the presence of 10 μg/ml polybrene. We used polybrene for viral infection, because MLV infections are usually carried out in the presence of polybrene to enhance infection. After 72 h, viral production was evaluated by measuring virion-associated reverse transcriptase (RT) activities in the culture supernatants.

Pre-incubation of the viruses with heparin at concentrations greater than 1 μg/ml resulted in a dose-dependent decrease in viral production (Fig. 1A). The 50% inhibitory dose (ID_{50}) values of heparin for F-, A8, and PVC-211 MLVs were 12.7 ± 4.5, 8.5 ± 0.9, and 13.0 ± 3.3 μg/ml, respectively; these values were not significantly different (Table 1). The structure of the most common disaccharide unit of heparin is composed of 2-*O*-sulfated iduronic acid and 6-*O*-sulfated, *N*-sulfated glucosamine (Fig. 1E). To investigate whether differences in the sulfation patterns of heparin affect the ability to inhibit ecotropic MLV infection, we pre-incubated viruses with a heparin derivative: NAdOS-H, which has markedly diminished *N*-sulfation and no *O*-sulfation; NA-H, which has diminished *N*-sulfation; or dNS-H, which completely lacks *N*-sulfation. NAdOS-H did not show inhibitory effects on infection of NIH 3T3 cells with F-, A8, or PVC-211 MLV even at a concentration of 1000 μg/ml (Fig. 1B and Table 1). In contrast, NA-H inhibited production of F-, A8, and PVC-211 MLVs in infected NIH 3T3 cells, with ID_{50} values of 54.5 ± 4.1, 62.1 ± 2.5, and 53.7 ± 2.8 μg/ml, respectively (Fig. 1C and Table 1); these values were significantly higher than for heparin ($P<0.001$). dNS-H also inhibited infection of NIH 3T3 cells with F-, A8, and PVC-211 MLVs, with ID_{50} values of 76.8 ± 3.9, 65.4 ± 2.3, and 72.4 ± 4.2 μg/ml, respectively (Fig. 1D and Table 1). The ID_{50} values for dNS-H were significantly higher than those of heparin ($P<0.001$).

Preparation of vesicular stomatitis virus (VSV)-based pseudotyped viruses carrying ecotropic MLV Env

Previous studies suggested that heparin affects ecotropic MLV infection during the early steps of viral replication. We used pseudotyped viruses bearing Env to analyze the effects of heparin on the viral replication process from the attachment to gene expression steps. We also sought to clarify the contribution of Env of ecotropic MLV to the inhibitory effects of heparin against viral infectivity by examining this response in the absence of other retroviral proteins, such as Gag and Pol, that might influence heparin-mediated reduction in infectivity. To this end, we prepared VSV based-pseudotyped viruses carrying the Env of F-, A8, or PVC-211 MLV (VSV/F-Env, VSV/A8-Env, and VSV/PVC-211-Env, respectively) using 293T cells.

Initially, we performed a Western blot analysis using an anti-Env antibody to examine whether Env protein is normally expressed in the 293T cells transfected with F-, A8-, and PVC-211-Env expression vectors, and compared the expression levels of Env in these cells. In the transfected 293T cells, the primary product observed was gp70, although gpr85 was also detectable (lanes 1–3 in Fig. 2). The expression levels of Env protein were similar in cells transfected with F-, A8-, and PVC-211-Env expression vectors. The Env-expressing cells were infected with recombinant VSV, which has the green fluorescence protein (GFP) gene in place of the viral G protein gene, and VSV-pseudotyped viruses carring Env were obtained. As a control, VSV viruses-like particles lacking Env (VSV/ΔEnv) were also obtained as described in the Materials and methods section. Next, we compared the amount of Env protein packaged in VSV-pseudotyped viruses among VSV/F-Env, VSV/A8-Env, and VSV/PVC-211-Env. In total, 2×10^5 infectious units of VSV/F-Env, VSV/A8-Env, and VSV/PVC-211-Env were spun down and the precipitates were used in a Western blot analysis. With regard to viral particles, gp70 was observed, and the amount of Env protein showed no appreciable differences among the virions (lanes 5–7 in Fig. 2).

Inhibitory effects of heparin and its derivatives on the infectivity of VSV-based pseudotyped viruses carrying ecotropic MLV Env

We examined the inhibitory effects of heparin and its derivatives on the infectivity of VSV-based pseudotyped viruses carrying ecotropic MLV Env. VSV/F-Env, VSV/A8-Env, and VSV/PVC-211-Env were pre-incubated with various concentrations of heparin, or a derivative, in the absence of polybrene, and then inoculated onto NIH 3T3 cells at an MOI of 1 in the presence of 10 μg/ml polybrene. After 16 h, GFP-positive cells were counted by fluorescence-activated cell sorting (FACS) in order to evaluate viral infectivity. Heparin was found to inhibit infection of NIH 3T3 cells with VSV/F-Env, VSV/A8-Env, and VSV/PVC-211-Env (Fig. 3A) with ID_{50} values of 7.0 ± 0.3, 8.0 ± 0.3, and 7.4 ± 0.4 μg/ml, respectively (Table 2). Although NAdOS-H did not inhibit infectivity of VSV/F-Env, VSV/A8-Env, or VSV/PVC-211-Env on NIH 3T3 cells (Fig. 3B and Table 2), high concentrations of NA-H or dNS-H did show inhibition of infection of NIH 3T3 cells (Figs. 3C and D). The ID_{50} values of NA-H (50.1 ± 3.9, 53.4 ± 2.6, and 50.8 ± 3.7 μg/ml for VSV/F-Env, VSV/A8-Env, and VSV/PVC-211-Env, respectively) and of dNS-H (67.8 ± 1.5, 64.8 ± 2.0, and 71.5 ± 1.8 μg/ml for VSV/F-Env, VSV/A8-Env, and VSV/PVC-211-Env, respectively) were significantly higher than those of heparin ($P<0.001$) (Table 2).

We also sought to compare the effects of heparin and its derivatives on the infectivity of ΔEnv-VSV-pseudotyped viruses. However, the efficiency of GFP gene transduction of the cells with the ΔEnv-VSV-pseudotyped viruses was too low to allow a reliable comparison to be carried out.

SPR analysis of the direct interactions of ecotropic MLV Env with heparin or its derivatives

In order to analyze direct interactions between Env and heparin, we measured the binding activities of VSV/F-Env, VSV/A8-Env, and

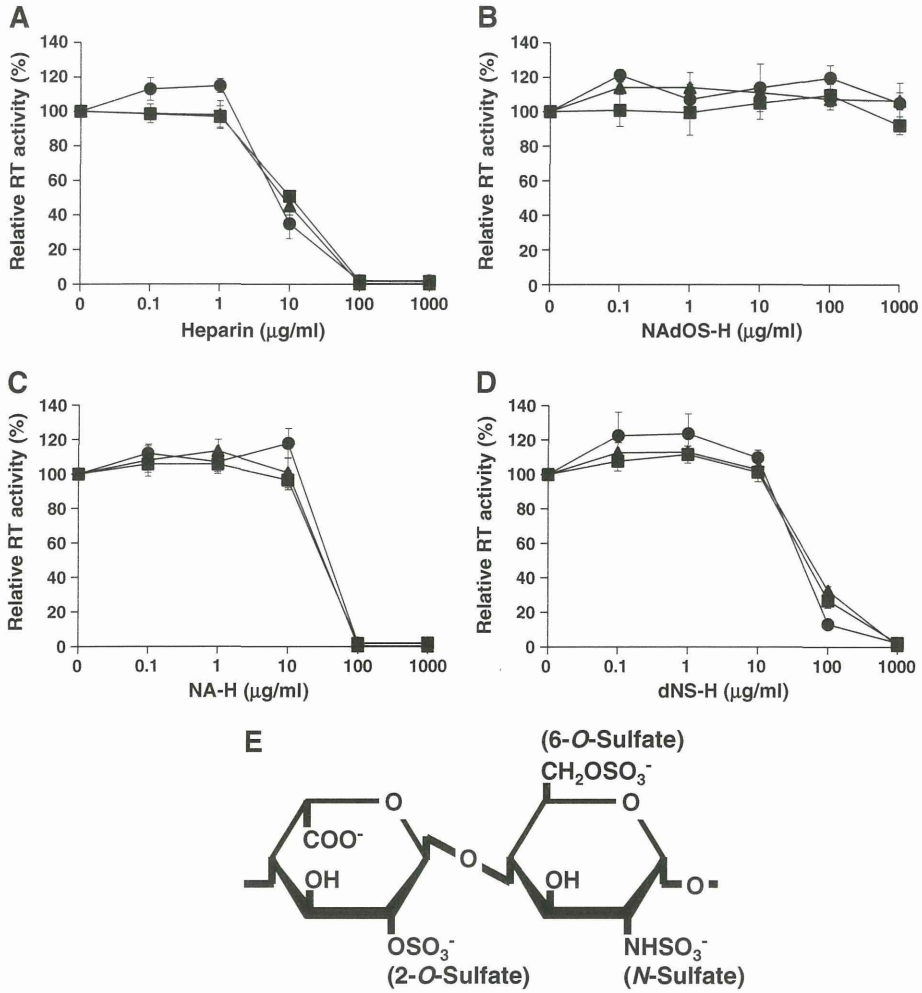

Fig. 1. Inhibitory activities of heparin and three derivatives against production of retroviruses in NIH 3T3 cells. F- (triangle), A8 (circle), and PVC-211 (square) MLVs were pre-incubated with various concentrations of heparin (A), NAdOS-H (*N*-acetyl-de-*O*-sulfated heparin) (B), NA-H (*N*-acetylheparin) (C), or dNS-H (de-*N*-sulfated heparin) (D) for 1 h at 37 °C in the absence of polybrene. The virus–heparin mixture was then inoculated onto NIH 3T3 cells in the presence of 10 μg/ml polybrene. After incubation for 1 h at 37 °C, the cells were washed three times with FCS-free DMEM and fresh culture medium was added. After 72 h, virion-associated RT activity in the culture supernatants was measured by an RT assay as described in the Materials and methods section. The mean values of 4 independent experiments and SEM are shown. (E) Schematic diagram of the major disaccharide repeating units of heparin. The most common disaccharide unit of heparin is composed of 2-*O*-sulfated iduronic acid and 6-*O*-sulfated, *N*-sulfated glucosamine.

VSV/PVC-211-Env to a heparin-immobilized chip (Heparin chip) by SPR. The SPR analyses were performed in the absence of polybrene; this protocol was adopted because in the experiments on inhibition of viral infection by heparin (Figs. 1 and 3), the viruses were pre-incubated with heparin in the absence of polybrene. Two different preparations of each pseudotyped virus were used for the analysis.

Table 1
ID_{50} of heparin and three derivatives against infection of MLVs into NIH 3T3 cells.

Reagents	Viruses		
	F	A8	PVC-211
Heparin	12.7 ± 4.5[a]	8.5 ± 0.9[a]	13.0 ± 3.3[a]
NAdOS-H	> 1000	> 1000	> 1000
NA-H	54.5 ± 4.1	62.1 ± 2.5	53.7 ± 2.8
dNS-H	76.8 ± 3.9	65.4 ± 2.3	72.4 ± 4.2

ID_{50} values (μg/ml) were calculated from the data shown in Fig. 1. The mean values (and SEMs) of 4 independent experiments are shown. Statistical comparison was performed using the t test. NAdOS-H: *N*-acetyl-de-*O*-sulfated heparin; NA-H:*N*-acetyl-heparin; dNS-H: de-*N*-sulfated heparin.

[a] $P < 0.001$ vs NA-H and dNS-H in each virus.

Env-deficient VSV-like particles (VSV/ΔEnv) and culture supernatant from 293T cells (Mock) were used as negative controls. Typical sensorgrams of the binding of the samples to the Heparin chip are shown in the top column of Fig. 4A. The flow of the viral particles, at various concentrations, across the Heparin chip was started at 0 s, and flow of the washing buffer was started at 300 s. Since the binding of virus to the Heparin chip appeared to reach equilibrium at 450 s, the Δdeg value at 450 s was selected as reflecting binding activity and plotted as shown in the top column of Fig. 4B. The results indicated that VSV-based pseudotyped viruses were bound to the Heparin chip in a dose-dependent manner. The binding activities of VSV/A8-Env and VSV/PVC-211-Env were clearly higher than that of VSV/F-Env, which exhibited higher binding activity than the negative controls. When viruses were saturated with heparin prior to SPR analysis, binding to the Heparin chip was inhibited (data not shown).

The binding activities of the VSV-based pseudotyped viruses to NAdOS-H or dNS-H immobilized on SPR sensor chips (NAdOS-H or dNS-H chips, respectively) were also examined (middle and bottom columns of Figs. 4A and B). We found that VSV-based pseudotyped viruses showed dose-dependent binding to the NAdOS-H or dNS-

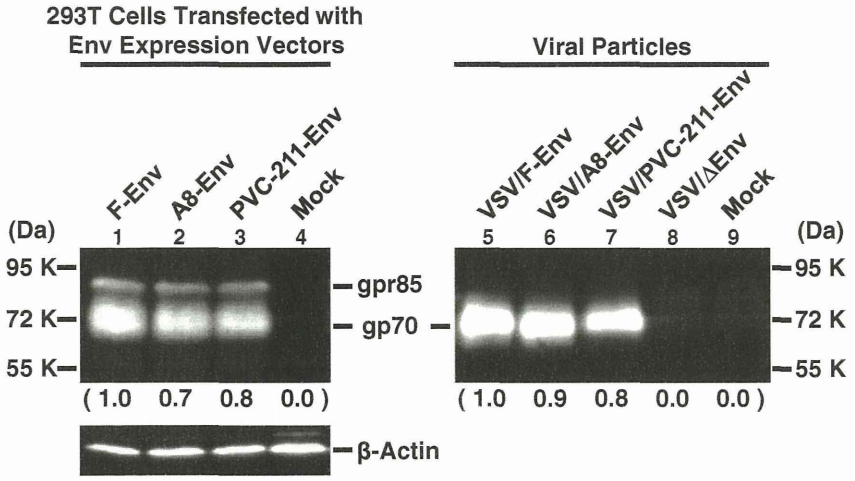

Fig. 2. Western blot analysis of the expression levels of Env in 293T cells transfected with Env expression vectors and VSV-pseudotyped virus particles. Lanes 1–3: 293T cells transfected with Env expression vectors. Lane 4: Mock-transfected 293T cells. Lanes 5–7: VSV-pseudotyped virus particles carring Env. 2×10^5 infectious units of viruses were applied to the Western blot. Details are given in the Materials and methods section. Lane 8: Env-deficient VSV-like particles prepared as described in the Materials and methods section. Lane 9: culture supernatant from 293T cells (used in the SPR analysis as a Mock control) was prepared as described in the Materials and methods section. To detect the Env protein, anti-SU (gp70) was used. Relative amount of Env protein is shown in parentheses. The expression levels of Env protein of transfected 293T cells were normalized against the intensity of the beta-actin band and are shown relative to the cell transfected with F-Env expression vector. The amount of Env protein in virions is shown relative to the VSV/F-Env. This figure is representative of repeat experiments. Experiments with each sample were performed twice and similar results were obtained.

H chips. The binding activities of VSV/A8-Env and VSV/PVC-211-Env to NAdOS-H or dNS-H were higher than those of VSV/F-Env. The binding activities of VSV/A8-Env and VSV/PVC-211-Env to NAdOS-H were clearly lower than those to heparin, but were similar or slightly lower than those to dNS-H. The binding activities of VSV/F-Env to NAdOS-H were slightly lower than those to heparin, and were not significantly different to those for dNS-H. Although NAdOS-H did not show any detectable inhibition of the infectivity of ecotropic MLV or VSV-based pseudotyped viruses carrying ecotropic Env, the binding activities of VSV/F-Env, VSV/A8-Env, and VSV/PVC-211-Env to this ligand appeared to be comparable to those to dNS-H.

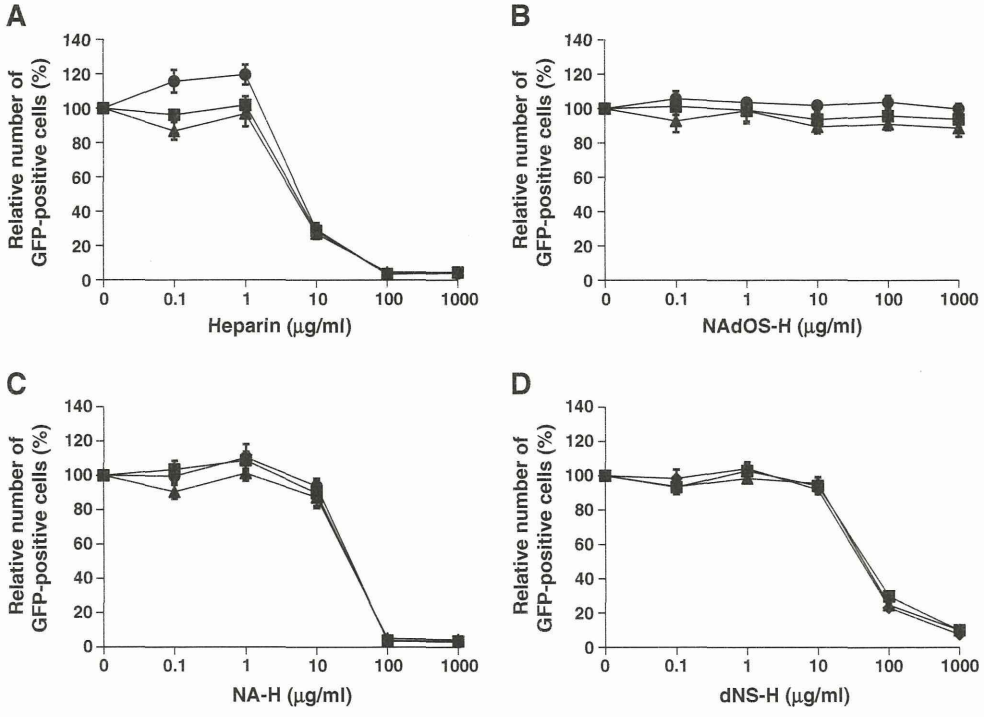

Fig. 3. Inhibitory activities of heparin and three derivatives against infection of VSV based-pseudotyped viruses carrying Env into NIH 3T3 cells. VSV/F-Env (triangle), VSV/A8-Env (circle), and VSV/PVC-211-Env (square) were pre-incubated with various concentrations of heparin (A), NAdOS-H (*N*-acetyl-de-*O*-sulfated heparin) (B), NA-H (*N*-acetylheparin) (C), or dNS-H (de-*N*-sulfated heparin) (D) for 1 h at 37 °C in the absence of polybrene. Then the virus–heparin mixture was inoculated onto NIH 3T3 cells in the presence of 10 μg/ml polybrene. After 16 h, GFP-positive cells were counted by FACS analyses. The mean values of 4 independent experiments and SEM are shown.

Author's personal copy

Table 2
ID_{50} of heparin and three derivatives against infection of VSV based-pseudotyped viruses carrying Env of MLV into NIH 3T3 cells.

Reagents	VSV based-pseudotyped viruses		
	VSV/F-Env	VSV/A8-Env	VSV/PVC-211-Env
Heparin	7.0 ± 0.3[a]	8.0 ± 0.3[a]	7.4 ± 0.4[a]
NAdOS-H	> 1000	> 1000	> 1000
NA-H	50.1 ± 3.9	53.4 ± 2.6	50.8 ± 3.7
dNS-H	67.8 ± 1.5	64.8 ± 2.0	71.5 ± 1.8

ID_{50} values (μg/ml) were calculated from the data shown in Fig. 3. The mean values (and SEMs) of 4 independent experiments are shown. Statistical comparison was performed using the *t* test. NAdOS-H: *N*-acetyl-de-*O*-sulfated heparin; NA-H:*N*-acetyl-heparin; dNS-H: de-*N*-sulfated heparin.
[a] $P<0.001$ vs NA-H and dNS-H in each virus.

Effect of polybrene on heparin-induced inhibition of MLV infection

In order to determine the effect of polybrene on the inhibitory activity of heparin against MLV infection, we performed experiments in the presence and absence of polybrene. Firstly, we examined the effects of polybrene on MLV infection at an MOI of 1. In the absence of polybrene, at 72 h post-infection, viral production of MLVs was undetectable level by an RT assay; at 96 h post-infection, viral production was detectable but was 10- to 50-fold lower than in the presence of polybrene (data not shown). In the presence of polybrene, viral production at 96 h post-infection was higher than at 72 h post-infection. Therefore, we evaluated viral production at 96 h post-infection in the following experiment. F-, A8, and PVC-211 MLVs were pre-incubated with various concentrations of heparin in the absence of polybrene, and then inoculated onto NIH 3T3 cells at an MOI of 1 either in the presence of 10 μg/ml polybrene or in its absence; viral production was evaluated at 96 h. In the presence of polybrene, the ID_{50} values of heparin for F-, A8, and PVC-211 MLVs were 44.4 ± 6.7, 47.9 ± 0.8, and 49.6 ± 2.2 μg/ml, respectively; these values were not significantly different (Fig. 5A and Table 3). The ID_{50} values in this experiment are higher than those shown in Fig. 1A and Table 1 due to differences in culture time; nevertheless, the inhibition curves in Fig. 5A are similar to those in Fig. 1A. In the absence of polybrene, the ID_{50} values of heparin for F-, A8, and PVC-211 MLVs were 0.56 ± 0.08, 0.61 ± 0.10, and 0.60 ± 0.05 μg/ml, respectively (Fig. 5B and Table 3); these values are not significantly different. However, these values are significantly lower than those in the presence of polybrene ($P<0.001$).

We also attempted to examine the effects of polybrene on the inhibitory activity of heparin against infection of NIH 3T3 cells by VSV-pseudotyped viruses. However, the efficiency of GFP gene transduction of the cells with the pseudotyped viruses in the absence of polybrene was too low to allow the effects of heparin to be reliably compared (data not shown).

Discussion

Soluble GAGs, such as heparin, have been shown to inhibit infection by MLV (Guibinga et al., 2002; Jinno-Oue et al., 2001; Walker et al., 2002). It has been reported that this inhibitory effect is determined by a number of factors: GAG concentration; electrostatic charge on the GAG; the affinity of the virus to the GAG; the cells from which the viruses are produced; and the cell type infected with the viruses. In this study, we examined the effects of soluble GAGs on the ability of ecotropic MLVs produced by NIH 3T3 cells to infect NIH 3T3 cells. Jinno-Oue et al. (2001) showed that, in the absence of polybrene, low concentrations of heparin (up to 100 μg/ml) enhanced the infectivity of F- and PVC-211 MLVs, whereas higher concentrations inhibited infectivity. In contrast, we found that 0.1 μg/ml of heparin did not affect the infectivity of F-, A8, and PVC-211 MLVs in the absence of polybrene; however, concentrations greater than 1 μg/ml, heparin inhibited infectivity (Fig. 5B). In the presence of polybrene, we found that 1 μg/ml or less of heparin did not affect the infectivity of F-, A8, and PVC-211 MLVs; at concentrations greater than 10 μg/ml, however, heparin inhibited infectivity in a dose-dependent manner (Figs. 1A and 5A). The apparent lack of any enhancing effects of heparin on ecotropic MLV infectivity in the present study may be due to differences in experimental conditions. Thus, the discrepant results in this and the previous study might be a consequence of using different cell types in which to measure viral infectivities. Jinno-Oue et al. (2001) used Rat-1 and primary rat brain capillary endothelial cells (BCEC) as target cells, while we used mouse NIH 3T3 cells.

Walker et al. (2002) and Guibinga et al. (2002) reported that the cell surface attachment of Env-deficient retrovirus-like particles was inhibited by heparin, suggesting that heparin inhibits Env-independent interaction of MLV with target molecules on the cell surface. By contrast, Jinno-Oue et al. (2001) showed that subtle changes in the Env protein amino acid sequences, which generated a heparin-binding site(s), could affect the heparin-binding affinity of the viruses and the susceptibility of the viruses to the effects of heparin. Thus, it is likely that heparin influences not only Env-independent attachment, but also Env-dependent attachment of the virus to the cell surface. In our present study, the binding to heparin by VSV-based pseudotyped viruses carrying the Env of F-, A8, or PVC-211 MLVs was quantitatively examined by SPR analysis. To our knowledge, the present study is the first to quantitatively compare heparin binding activities of Env of different ecotropic MLVs using SPR technology. Our results indicated that the binding activities of VSV based-pseudotyped viruses carrying the Env of ecotropic MLVs were higher than that of the Env-deficient virus-like particle, and that the Env sequence influenced the binding activity of the pseudotyped viruses to heparin (Figs. 4 and 6). Therefore, the results strongly suggest that the Env per se of these ecotropic MLVs can directly interact with heparin. PVC-211-Env exhibited the highest heparin binding activity, followed by A8-Env, and then F-Env (Fig. 4). These results are consistent with those of a previous study in which heparin agarose was used to assess the heparin binding activities of F-MLV and PVC-211 MLV (Jinno-Oue et al., 2001). F-Env, which showed the lowest binding activity to heparin, had 26 amino acid substitutions compared to A8-Env (Fig. 6). By contrast, A8-Env and PVC-211-Env showed similar binding activities and differed by only 3 amino acids (Fig. 6). The consensus sequences for the heparin-binding domain (HBD) are XBBXBX and XBBBXXBX, where X represents any amino acid and B indicates a basic amino acid (Cardin and Weintraub, 1989). A stretch of 6 amino acids from Ser^{124} to Glu^{129} in the receptor-binding domain (RBD) of F-Env constitutes a putative HBD. However, a previous study suggested that this sequence did not function as an HBD (Jinno-Oue et al., 2001). Compared to F-Env, the substitution of Glu^{129} by Lys in PVC-211-Env generated an additional, overlapping HBD from Pro^{127} to Ser^{132}. This new HBD has been suggested to contribute to the high binding ability of PVC-211 MLV for heparin. Intriguingly, the amino acids at positions 124 to 132 of A8-Env are identical to those of F-Env, and thus A8-Env has only one putative HBD that might not be functional. Therefore, the number of HBDs cannot explain the difference in binding activities of A8-Env and F-Env to heparin. Recently, the heparin binding activities of wild-type and mutant gp120 of HIV-1 were studied using SPR-based binding assays (Crublet et al., 2008). Four new HBDs were identified in the V2 and V3 loops, in the C-terminal domain, and within the CD4-induced bridging sheet. Three of these HBDs were found in domains of the protein that are involved in co-receptor recognition. In particular, Arg^{419}, Lys^{421}, and Lys^{432}, which directly interact with the co-receptor, are targeted by heparin, suggesting that these basic amino acids are important for the interaction with heparin. In contrast to F-Env, which has Gln^{61} and Ser^{80} in the variable region A (VRA) of RBD, both A8-Env and PVC-211-Env have Arg^{61} and Arg^{80} in common (Fig. 6). Therefore, we suggest that

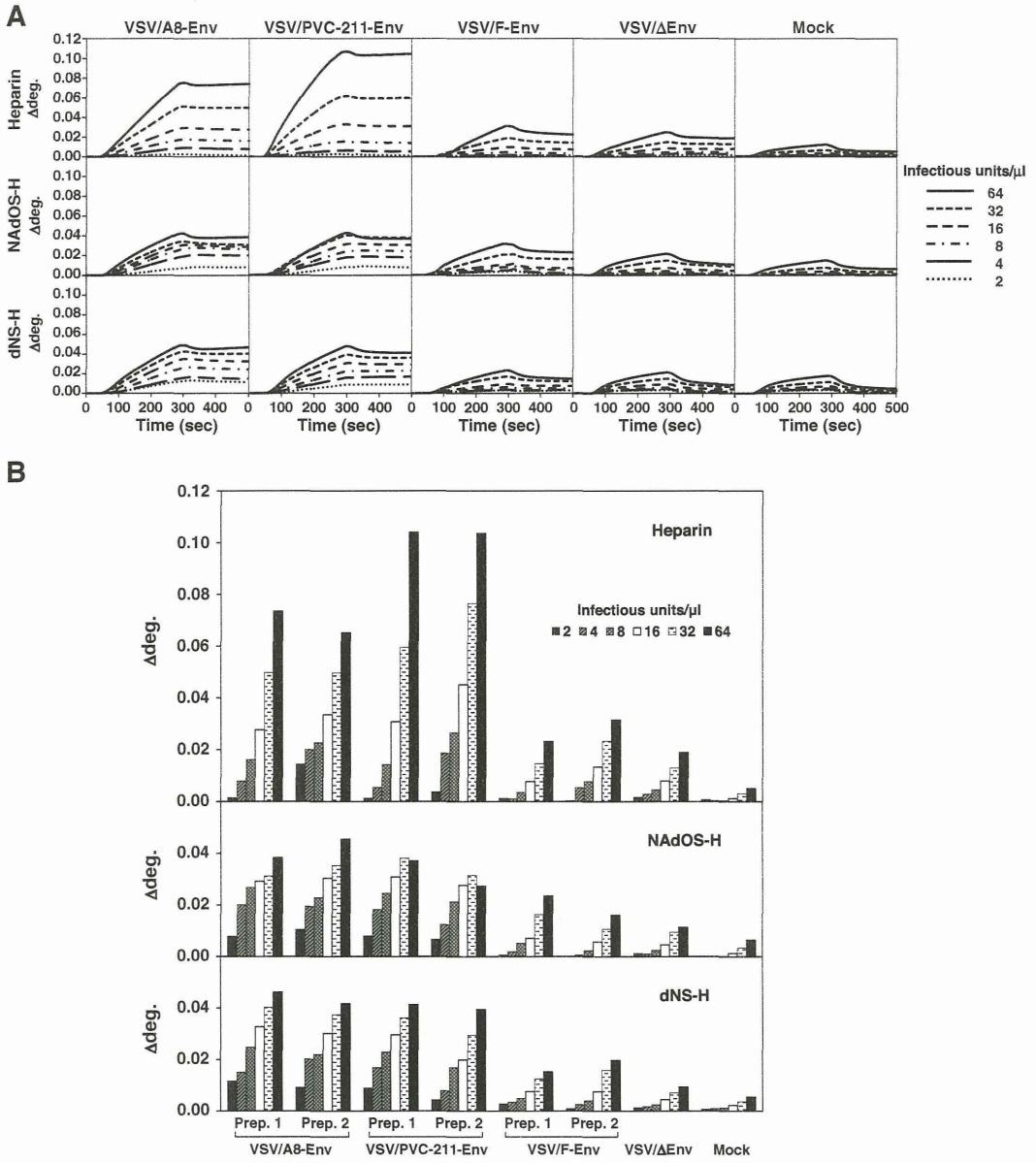

Fig. 4. SPR analysis of the binding of VSV based-pseudotyped viruses carrying Env of F- (VSV/F-Env), A8 (VSV/A8-Env), or PVC-211 MLV (VSV/PVC-211-Env) to heparin, NAdOS-H (*N*-acetyl-de-*O*-sulfated heparin), or dNS-H (de-*N*-sulfated heparin) immobilized on SPR sensor chips. Two independent preparations (Prep. 1 and Prep. 2) of VSV/F-Env, VSV/A8-Env, and VSV/PVC-211-Env were tested. (A) SPR sensorgrams of viral particles of Prep. 1 for the Heparin chip, the NAdOS-H chip, or the dNS-H chip. (B) The equilibrium level of binding of viral particles to the Heparin chip, the NAdOS-H chip, or the dNS-H chip at 450 s. VSV/ΔEnv: Env-deficient VSV-like particles; Mock: culture supernatants of 293T cells. 1×10^6 infectious units of VSV based-pseudotyped viruses carrying Env were prepared and treated for SPR analysis as described in the Materials and methods section. VSV/ΔEnv and Mock controls were prepared as described in the Materials and methods section. The aliquots from both controls were equivalent in volume to those from the culture supernatants of VSV/Env-producing cells, which contained 1×10^6 infectious units, and were treated in the same manner.

these two residues in A8- and PVC-211-Env might contribute to the higher heparin-binding activity. Furthermore, Lys^{129} is present only in PVC-211-Env and may be responsible for the additional heparin-binding activity.

Although PVC-211-Env had the highest heparin binding activity, followed by A8-Env, and then F-Env (Fig. 4), the ID_{50} values of heparin for infection by PVC-211, A8, or F-MLV were not significantly different (Fig. 1 and Table 1). Similarly, the ID_{50} values of heparin for infection of VSV-based pseudotyped viruses bearing PVC-211-, A8-, or F-Env were not significantly different (Fig. 3 and Table 2). The reasons why the estimates for inhibition of viral infection do not correlate with those from the SPR analyses are not clear, but the following possibilities could be suggested. First, the relatively low binding activity of Env to heparin, which was observed in the SPR analysis of F-Env, might be sufficient to block viral infection. Second, the SPR analysis might be more sensitive to heparin-binding activity than the inhibition assay of viral infectivity. In the SPR analysis, viral particles bind to heparin immobilized to a chip, and then excess and low-affinity viral particles are washed out. In contrast, in the inhibition assay, small soluble molecules of heparin bind to the Env of viruses, and thus relatively low-affinity binding between heparin and Env could have a significant effect on viral